ATRQβ-001 Vaccine Prevents Experimental Abdominal Aortic Aneurysms

Hongrong Zhang, PhD;* Mengyang Liao, PhD;* Mingsi Cao, MSc;* Zhihua Qiu, PhD; Xiaole Yan, PhD; Yanzhao Zhou, PhD; Hailang Wu, PhD; Yingxuan Wang, PhD; Jiayu Zheng, PhD; Jiaxing Ding, MSc; Min Wang, PhD; Yuhua Liao, PhD; Xiao Chen, PhD

Background—We have developed a peptide vaccine named ATRQβ-001, which was proved to retard signal transduction initiated by angiotensin II (Ang II). Ang II was implicated in abdominal aortic aneurysm (AAA) progression, but whether the ATRQβ-001 vaccine would prevent AAA is unknown.

Methods and Results—Ang II-infused ApoE$^{-/-}$ mice and calcium phosphate-induced AAA in C57BL/6 mice were used to verify the efficiency of ATRQβ-001 vaccine in AAA. Results demonstrated that the vaccine effectively restrained the aneurysmal dilation and vascular wall destruction of aorta in both animal models, beyond anti-hypertensive effects. In Ang II-induced AAA vascular sections, Immunohistochemical staining showed that the vaccine notably constrained vascular inflammation and vascular smooth muscle cell (VSMC) phenotypic transition, concurrently reduced macrophages infiltration. In cultured VSMC, the anti-ATR-001 antibody inhibited osteopontin secretion induced by Ang II, thereby impeded macrophage migration while co-culture. Furthermore, metalloproteinases and other matrix proteolytic enzymes were also found to be limited by the vaccine in vivo and in vitro.

Conclusions—ATRQβ-001 vaccine prevented AAA initiation and progression in both Ang II and calcium phosphate-induced AAA models. And the beneficial effects were played beyond decrease of blood pressure, which provided a novel and promising method to take precautions against AAA. (*J Am Heart Assoc.* 2019;8:e012341. DOI: 10.1161/JAHA.119.012341.)

Key Words: abdominal aortic aneurysm • angiotensin receptor • matrix metalloproteinases • vaccine

Abdominal aortic aneurysm (AAA) is a life-threatening disease relatively common in elderly people. Population-based studies in adults older than 50 years demonstrated that the prevalence of AAA is 3.9% to 7.2% in men and 1.0% to 1.3% in women, and the incidence may be increasing.[1,2] People with AAAs are often undetected until the rupture, because they can be entirely asymptomatic. However, current therapeutic options to prevent rupture are restricted to surgical repair and not everyone is suitable to the surgery.[3] In patient with small aneurysms (<5.0 cm), early surgery did not result in any long-term survival advantages[4,5] and it lacks of validated pharmaceutical approaches yet.[6] As a result, it's urgent to seek for alternative avenues to limit the aneurysm initiation and progression.

Interferences with renin–angiotensin-aldosterone system are always drawing researchers' attention on account of the angiotensin II (Ang II)-induced AAA model, which was well-established to recapitulate many features of human AAA, including elastin breaks, extracellular matrix degradation, intraluminal thrombus, inflammatory cell accumulation, and aortic rupture. In Ang II or elastase-induced AAA models, aortic dilation was almost completely abrogated by angiotensin II type 1a receptor knockout.[7,8] What's more, Ang II-forming activity and Ang II-forming enzymes were strikingly upregulated in human aortic aneurysm specimens.[9–11] All these implied the importance of Ang II in the process of AAA.

We had developed a peptide vaccine named ATRQβ-001 vaccine, which targeted at the second extracellular loop of the human angiotensin II type 1 receptor (AT1R). Previous researches suggested that the ATRQβ-001 vaccine suppressed AngII-AT1R activation and ameliorated relevant pathological injuries in hypertension, diabetic nephropathy,

<div style="border: 2px solid red;">

Clinical Perspective

What Is New?

- This is the first report showing that ATRQβ-001 vaccine, a virus-like particle–based anti-hypertensive vaccine aimed at angiotensin II type 1 receptor, could effectively impede abdominal aortic aneurysm initiation and progression in both angiotensin II and calcium phosphate-induced abdominal aortic aneurysm models.

What Are the Clinical Implications?

- It was noteworthy that immunization of the ATRQβ-001 vaccine prevented aneurysm and minimized administration frequency without affecting normal blood pressure, which indicated that ATRQβ-001 vaccine may serve as a promising avenue to prevent aneurysm.

</div>

and atherosclerosis.[12–14] In ApoE$^{-/-}$ mice maintained with western diet, the ATRQβ-001 vaccine was found to promote stability of the atheromatous plaque and mitigated accumulation of macrophages.[14] We speculated that the vascular protective effect of ATRQβ-001 vaccine would sustain in AAA milieu. In this study, we used 2 different AAA models to ascertain the effectiveness of the ATRQβ-001 vaccine and illustrated the underlying mechanisms.

Methods

The data that support the findings of this study are available from the corresponding author upon reasonable request.

Peptide Synthesis and Monoclonal Antibody Preparation

The ATR-001 peptide, with the amino acids sequence C-A-F-H-Y-E-S-Q (CQ8) corresponding to the sequence of the second extracellular loop of the human AT1R position 180–187, was synthesized by GL Biochem Ltd (Shanghai, China). The purity was >98% and was determined using high-performance liquid chromatography and mass spectrometry.

The monoclonal anti-ATR-001 antibody was customized and identified via ELISA tests. Briefly, male BALB/C mice aged 6-week-old (n=6) were subcutaneously immunized with the ATR-001 peptide 50 μg on day 0, 21, 35 and then strengthen-immunized intraperitoneally on day 49. Serums of those mice were collected for ELISA meanwhile. On day 54, spleen cells of mouse bearing the highest antibody titer were harvested to hybridize with myeloma cell line SP2/0 for hybridoma. Planking hybridomas that produced positive antibodies in cell culture supernatant to 96-well plates, single positive

hybridoma was selected. The monoclonal hybridoma was amplificated and intraperitoneally injected to mice. One week later, the ascites was collected and purified to get monoclonal antibody. Affinity of the antibody was identified by ELISA test with ATR-001 peptide-linked plates.

Vaccine Preparation

The ATRQβ-001 vaccine was prepared as previously described.[12] Briefly, prokaryotic expression plasmid that express Qβ virus-like particle (VLP) was constructed and then transfected into BL21 *Escherichia coli*. The expressed Qβ VLP protein was collected, purified and identified according to corresponding route. The ATR-001 peptide was covalently conjugated to Qβ VLPs via the Sulfo-SMCC crosslinker (Pierce) to produce the ATRQβ-001 vaccine. Quality of the vaccine was identified by SDS-PAGE and concentration was determined using Bradford protein assay kit (Pierce).

Mouse Model of Aneurysm and Treatment

Male ApoE$^{-/-}$ mice on C57BL/6 background and male C57BL/6 mice were purchased from Beijing Huafukang Bioscience Co Inc (Beijing, China), kept in the Experimental Animal Center of Tongji Medical College of Huazhong University of Science and Technology (Wuhan, China) in a specific pathogen-free environment. All experiments and animal care were performed in accordance with the guidelines of the animal care and use ethical committee of Tongji Medical College, Huazhong University of Science and Technology. The protocol was approved by Animal Care and Use Committee of Hubei Province. Sterile water and standard chow diet were ad libitum feeding. Body weights of animals were recorded every week.

For the Ang II-infusion AAA model, male ApoE$^{-/-}$ mice aged 10 weeks were randomly assigned to 6 groups, receiving 4-week infusions of saline vehicle or solutions of Ang II (ENZO Biochem, ALX-151-039-M025) with osmotic minipumps. The groups as following: (1) the control group (n=8): 200 μL saline; (2) the Ang II group (n=23): Ang II (1.44 mg/kg per day) subcutaneous perfusion; (3) the telmisartan group (n=16): Ang II (1.44 mg/kg per day) subcutaneous perfusion and telmisartan (5 mg/kg per day) via oral gavage; (4) the vaccine group (n=21): Ang II (1.44 mg/kg per day) subcutaneous perfusion and ATRQβ-001 vaccine immunized subcutaneously 200 μg on day 0, 100 μg on days 14 and 28, respectively; (5) the Qβ group (n=20): Ang II (1.44 mg/kg per day) subcutaneous perfusion and Qβ VLP immunized subcutaneously 200 μg on day 0, 100 μg on day 14 and 28; (6) the hydralazine group (n=14): Ang II (1.44 mg/kg per day) subcutaneous perfusion and hydralazine (5 mg/kg per day) via oral gavage. All the animals

were subcutaneously implanted with 200 µL osmotic mini-pumps (model 2004; Alzet Osmotic pumps) at age 15-weeks (day 35) according to the instruction.[15] Animals were euthanized on 7 or 28 days after implantation.

For the calcium phosphate ($CaPO_4$)-induced AAA model (a modified calcium chloride model), Male 10-week-old C57BL/6 mice were randomly divided into 5 groups: Control group (n=11), $CaPO_4$ group (n=14), vaccine group (n=14), Qβ group (n=14), and anti-ATR-001 group (n=13). The vaccine group mice were vaccinated subcutaneously with ATRQβ-001 vaccine 200 µg on days 0, 100 µg on day 14 and 28, while the Qβ group were vaccinated with equivalent dosage of Qβ VLP correspondingly. The anti-ATR-001 group mice were injected 100 µg anti-ATRQβ-001 monoclonal antibody per 7 days via caudal veins since the operation. All 5 groups conducted operation on day 35 as described previously.[16] Briefly, under general anesthesia, the infrarenal region of the abdominal aorta was isolated and then applied perivascularly with a small piece of gauze soaked in 0.5 mol/L calcium chloride ($CaCl_2$). Ten minutes later, the $CaCl_2$-soaked gauze was replaced with another piece of PBS-soaked gauze for 5 minutes. The control group mice received 1 treatment of 0.5 mol/L sodium chloride (NaCl)-soaked gauze for 15 minutes accordingly. Four weeks after operation, all the animals were euthanized, and tissues were harvested.

Blood Pressure Measurement

Blood pressure and heart rate were recorded non-invasively in conscious animals, using a computerized tail-cuff system (BP 2010A, Softron, Japan). Mice were acclimatized to a dark chamber at 37°C for 15 minutes, subsequently transferred to a dark cage covered with a heating pad for monitoring. The blood pressure measurements were manipulated by 1 person who was masked to the grouping and averaged from 15 readings for each animal. All the measurements were performed in a quiet environment at 20°C to 25°C in the morning (from 9:00 AM to 11:00 AM).

Serum Lipids, Antibody Titer, and Cytokines Detection

Before blood collection, the animals were fasted for 12 hours. The sera were separated by centrifugation at a rate of 1000g for 10 minutes at room temperature. The serum lipids including total cholesterol, triglyceride, high-density lipoprotein, and low-density lipoprotein levels were measured via biochemical kits (BEIJIAN-XINCHUANGYUAN Bio-Tech Co, Ltd, Beijing, China). The serum antibody titers were detected by ELISA with ATR-001 peptide–linked plates on days 0, 6, 20, 34, 48, and 62, respectively. Serum concentration of

interleukin (IL)-1β and IL-6 were, respectively, detected by ELISA kit (NeoBioscience, EMC001b.96 and EMC004.96) according to instructions.

Tissue Preparation and Histological Assessment

Animals were normally euthanized at selected intervals by anesthesia. The heart and entire aorta were exposed and perfused with PBS, stripped off periadventitial tissue, then rapidly excised and photographed. Tissues for morphological and immunohistochemical observations were routinely fixed in 4% phosphate-buffered paraformaldehyde, subsequently embedded in paraffin, serially sectioned at 5 mm interval. The rest tissue samples were removed fresh and stored at −80°C until biochemical assays. The paraffin-embedded sections were stained with hematoxylin and eosin, Elastic Van Gieson, or Alizarin Red staining. Serial paraffin sections were also used for immunostaining using the following primary antibodies: anti-CD68 (Abcam, ab31630) for macrophages, anti-MMP2 (R&D System, AF1488), anti-MMP9 (R&D System, AF909), anti-extracellular MMP inducer (EMMPRIN) (Abcam, ab108317), anti-osteopontin (R&D System, AF808). All the images of stained sections were captured via Olympus biological microscope (Japan). Image of stained sections were quantified using ImageJ Software (National Institutes of Health, Bethesda, MD). Analysis was performed masked to the sample identity.

Immunofluorescence was performed on paraffin-embedded sections and slides of fixed cells climbing. The specimens were incubated with following primary antibodies: mouse anti-smooth muscle actin antibody (1:100; Sigma-Aldrich, A5228), rabbit anti-SM22alpha antibody (1:100; Abcam, ab14106), rabbit anti-AT1R (1:100; Abcam, ab124505) or mouse anti-ATR-001 antibody (10 µg/mL), respectively, then incubated with fluorescein-conjugated secondary antibodies (1:100 dilution; Invitrogen) and DAPI (Servicebio, Wuhan, China). All sections were observed under a laser confocal microscope (Nikon, Tokyo, Japan).

Cell Culture Assays

Mouse macrophage cell line Raw264.7 and mouse aorta vascular smooth cell line (MOVAS) were purchased from ATCC and cultured in Dulbecco Modified Eagle's Medium/High Glucose (DMEM/H) medium supplemented with 10% fetal bovine serum, 100 U/mL penicillin, and 100 mg/mL streptomycin. CHO-K1 stably expressing AT1R was purchased from PerkinElmer (Shanghai, China) and cultured in DMEM/F12 medium containing 10% fetal bovine serum, 100 U/mL penicillin, and 100 mg/mL streptomycin. All these cells are maintained at 37°C in a humidified 5% CO_2 incubator. For stimulation, MOVAS cells were pretreated with the anti-ATR-

001 antibody (10 μg/mL), telmisartan (1×10^{-6} mol/L), or the normal mouse immunoglobulin G (Santa Cruz Biotechnology, sc-2025) for 2 hours, respectively, subsequently stimulated by Ang II (1×10^{-5} mol/L) for 72 hours. And Raw264.7 cells were pretreated with the anti-ATR-001 antibody (10 μg/mL), telmisartan (1×10^{-6} mol/L), or the normal mouse immunoglobulin G for 2 hours, respectively, subsequently stimulated by Ang II (1×10^{-5} mol/L) for 24 hours.

Monocyte/Macrophage Migration Assay

The migration of monocytes/macrophages toward VSMC was assessed by Transwell chambers (Corning, USA) with 24-well tissue culture plates composed of 8-μm pore polycarbonate filters. MOVAS cells were serum-starved for 24 hours before Ang II (1×10^{-6} mol/L) or vehicle stimulation for an additional 72 hours. Confluent RAW264.7 were detached by 0.25% tripsin-EDTA, Gibco, NY, USA, 15050065, and re-suspended in DMEM/H medium containing 1% fetal bovine serum. The RAW264.7 cells suspensions (100 μL, $5\times10\,000$ cells) were then added into the upper chamber of transwells, and the lower chamber was filled with 500 μL of DMEM/H medium supplemented with 1% fetal bovine serum. The chambers were then incubated at 37°C for 12 hours in 5% CO_2 incubator. After incubation, the filters were rinsed with PBS and fixed in 4% paraformaldehyde for 30 minutes and stained with crystal violet for 20 minutes. Cells remaining on the upper surface were removed by gentle abrasion using a cotton bud, and cells on the underside (invaded cells) observed under the microscope. The mean number of cells on the lower surface was counted from 4 randomly chosen high-power fields ($\times100$) under an inverted fluorescence microscope (Nikon, TE-2000U) in 3 independent experiments. Data were calculated as the ratio against respective control groups.

Western Blot

Total proteins of cell samples were extracted with protein extraction buffer (Pierce) containing a protease inhibitor cocktail (Roche Applied Science). The homogenates were centrifuged at 15 294g for 15 minutes at 4°C to yield supernatant. Protein concentrations were confirmed via the BCA assay kit (Pierce). Equivalent amounts of the extracted protein were electrophoresed on 10% SDS polyacrylamide gels and then electro-transferred onto polyvinylidene fluoride membranes (Roche Applied Science). After blocked in 5% skim milk for 2 hours at room temperature, membranes were incubated with rabbit anti-AT1R (1:1000; Abcam, ab124505) primary antibody at 4°C overnight. Then the membranes were washed and incubated with secondary antibodies. The immunoreactive bands were finally detected by enhanced chemiluminescence reagent (Thermo Fisher Scientific).

Quantitative Real-Time Polymerase Chain Reaction

Total RNA was extracted from the tissue of the aorta or the treated cells via RNAioplus kit (Takara, Kyoto, Japan, RR9109), reversely transcribed with the cDNA Synthesis Kit (Takara, RR036A) and amplified with SYBR Premix Ex Taq Kit (Takara, RR420A) according to manufacturer's protocol. The expression of the associated genes was assessed by quantitative real-time polymerase chain reaction performed with a Step One Real-Time PCR machine (Applied Biosystems, Foster City, CA). Primers were showed in Table S1.

Statistical Analysis

Data were shown as the mean±SEM. Student t-test was used for comparisons between 2 groups and ANOVA with Bonferroni post test was used for comparisons between ≥3 groups.

Table. Animal Characteristics

Animal Characteristics	Control (n=8)	Ang II (n=23)	Telmisartan (n=16)	Hydralazine (n=14)	Vaccine (n=21)	Qβ (n=20)
Body weight, g	31.58±1.49	31.39±1.05	29.94±0.50	29.22±0.26	32.13±0.48	30.64±0.70
TC, mmol/L	11.33±0.95	11.22±0.91	11.33±0.73	11.61±0.63	11.11±0.63	11.29±0.73
Triglycerides, mmol/L	1.78±0.097	1.80±0.15	1.83±0.16	1.69±0.11	1.95±0.20	1.85±0.15
HDL cholesterol, mmol/L	3.89±0.33	4.52±0.32	4.74±0.32	5.00±0.28	4.03±0.32	4.78±0.34
LDL cholesterol, mmol/L	7.36±0.45	8.93±0.83	8.12±0.92	9.01±0.39	8.03±0.62	8.97±0.60
SBP, mm Hg	120.39±1.97[†]	161.07±2.45	135.25±3.40[†§]	140.37±3.09[†§]	147.52±1.74[*‡]	163.15±3.35
Heart rate, bpm	603.31±13.20	574.27±15.57	581.62±18.93	591.79±20.07	597.13±16.06	601.39±16.51

Data are expressed as mean±SEM. Ang II indicates angiotensin II; HDL, high-density lipoprotein cholesterol; LDL, low-density lipoprotein cholesterol; SBP, systolic blood pressure; TC, total cholesterol.
*$P<0.001$, †$P<0.0001$ vs angiotensin II.
‡$P<0.001$, §$P<0.0001$ vs Qβ.

Experiments involve serial assessments over time by group were measured by ANOVA for repeated measurement. The Fisher exact test was used for the incidence of aneurysm. And non-parametric test was used for severity of aneurysm analysis. Statistical analyses of the data were performed by GraphPad Prism 6.0 (GraphPad Software, San Diego, CA). $P<0.05$ was considered statistically significant (except Fisher exact test, in which the significant level was adjusted).

Result

ATRQβ-001 Vaccine Blocks Ang II-Induced AAA Formation and Progression Beyond Anti-Hypertensive Effect

We first conducted experiments to identify the activities of ATRQβ-001 vaccine on Ang II-induced AAA model. Male ApoE$^{-/-}$ mice were randomized to 5 groups, receiving saline vehicle or Ang II with osmotic minipumps. ATRQβ-001 vaccine was prepared and injected to the vaccine group mice ahead of minipumps implantation (Figure S1). No evidence of skin damages at the site of subcutaneous injection was noted in vaccine-treated animals. Apart from differentiated blood pressure, there was no significant difference between groups on body weight, lipid profiles, and heart rates (Table).

To ascertain the efficiency of ATRQβ-001 vaccine on exogenous Ang II, we evaluated the blood pressure and serum antibody titer against the ATR-001 peptide at scheduled intervals. Immunization with the ATRQβ-001 vaccine effectively limited the augment of blood pressure compared with the Ang II group (147.52 ± 1.74 mm Hg versus 161.07 ± 2.45 mm Hg, $P<0.001$) (Figure 1A), so did telmisartan and hydralazine (telmisartan 135.25 ± 3.40 versus 161.07 ± 2.45 mm Hg, $P<0.0001$; hydralazine 140.37 ± 3.09 versus 161.07 ± 2.45 mm Hg, $P<0.0001$). After the second injection, the mean of ATR-001-specific antibody titer peaked as 1:260 000, remained 1:230 000 after the third injection, and maintained above 1:10 000 throughout the course of the experiment (Figure 1B).

To evaluate the AAA formation and severity, we examined the morphology of aorta of every individual mouse. Persistent infusion of Ang II profoundly increased the external diameter of abdominal aorta and the occurrence of aneurysms, which was defined as an increase of >50% in native vessel diameter (Figure 1C through 1E). No AAA formation was observed in saline control group. Compared with the Ang II group, the incidence of AAA was reduced by 54.9% in the ATRQβ-001 vaccine group (33.3%, 7 of 21 versus 73.9%, 17 of 23, $P<0.05$), and by 74.6% in telmisartan group (18.75%, 3 of 16 versus 73.9%, 17 of 23, $P<0.001$). Meanwhile, the maximal aortic diameter was limited by ATRQβ-001 vaccine or telmisartan. When we

characterized aortic gross pathology using the classification of Daugherty and colleagues,[17,18] we found that only 19% of mice in the vaccine group displayed features of advanced AAA pathology with macroscopically visible thrombus (grade III–IV), contrasted to 47.8% in the Ang II group (Figure 1F). ATRQβ-001 vaccine also reduced the mortality rate attributable to aneurysm rupture compared with the Ang II group, although there was no statistical significance (Figure S2). Similarly, histological analysis of hematoxylin and eosin and Elastic Van Gieson staining showed that administration of ATRQβ-001 vaccine or telmisartan blunted the aneurysmal dilation and reserved the integrality of vascular wall, compared with the Ang II group mice (Figure 2). Neither did hydralazine nor Qβ VLP manifest protective effects against AAA.

ATRQβ-001 Vaccine Rescued CaPO$_4$-Induced Aorta Dilation and Tunica Media Calcification

To further confirm the ability of ATRQβ-001 vaccine to prevent aortic aneurysms, we used a modified calcium chloride (CaCl$_2$) model in the C57BL/6 background, the calcium phosphate (CaPO$_4$) model. CaCl$_2$ in combination with PBS accelerated aorta dilation, mainly rendered pathologic damages as elastin degradation and media calcification, with the blood pressure slightly increased (Figure 3A). Consistent with the findings observed in Ang II-infused ApoE$^{-/-}$ mice, the ATRQβ-001 vaccine availably inhibited the dilation of abdominal aortas (Figure 3B and 3C). Although systolic blood pressure was not significantly decreased by the vaccine, the Elastic Van Gieson staining of the aortic wall showed reduced fragmentation of the elastin layer in the immunized animals' aortas (Figure 3D). Alizarin Red staining for calcium deposition was also alleviated (Figure 3D). Moreover, to test the efficiency of anti-ATR-001 antibody, we used a group of mice injected with anti-ATR-001 monoclonal antibody on the CaPO$_4$-induced AAA model. Not surprisingly, administration of specific monoclonal antibody against the ATR-001 peptide (100 μg/week) resulted in similar protective effects with the ATRQβ-001 vaccine (Figure 3B and 3C), which strongly indicated the AT1R-dependend effect.

ATRQβ-001 Vaccine Ameliorated Vascular Inflammation and VSMC Phenotypic Transition

Given the fact that Ang II-infused ApoE$^{-/-}$ model is more commonly used and reproduces much more characteristics of human AAA compared with CaPO$_4$-induced AAA,[19] we focused on the former to investigate the underlying mechanisms. Firstly, we examined the effect of ATRQβ-001 vaccine on inflammatory response. Continuous perfusion of Ang II elevated the serum concentration of IL-1β and IL-6, which was
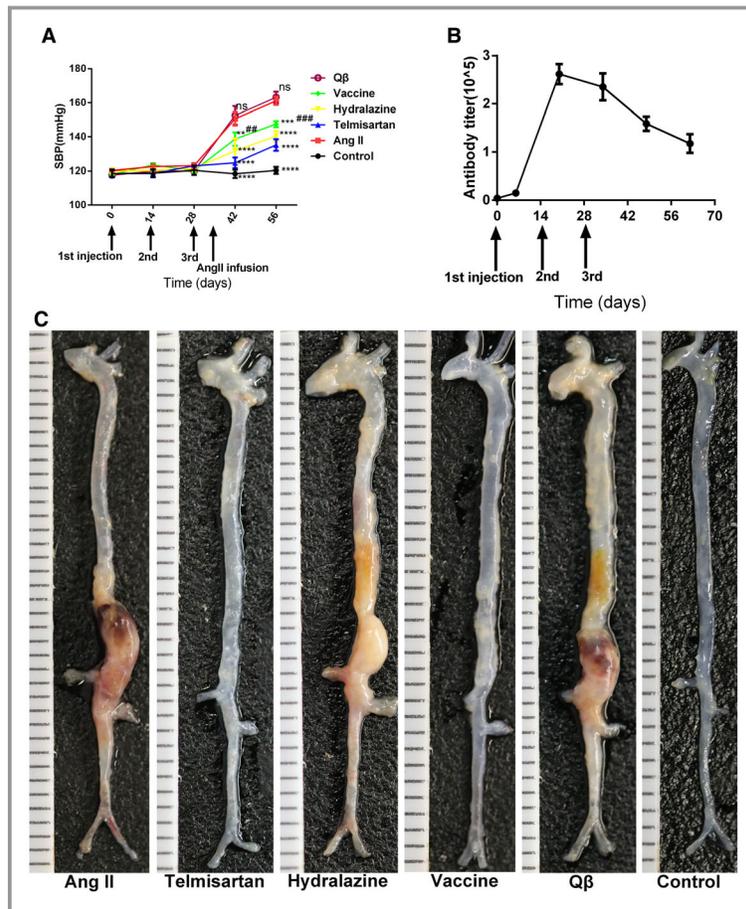
Figure 1. ATRQβ-001 vaccine prevented the blood pressure increase and aneurysm formation in Ang II-induced abdominal aortic aneurysm model. Male ApoE$^{-/-}$ mice were randomized to 5 groups, receiving saline vehicle or angiotensin II with osmotic minipumps. ATRQβ-001 vaccine was prepared and injected to the vaccine group mice ahead of minipumps implantation. The Qβ group were vaccinated with equivalent dosage of Qβ virus-like particle correspondingly. The serum antibody titers were detected by ELISA. **A**, The systolic blood pressure of ApoE$^{-/-}$ mice (n>5 per group). **P<0.01, ***P<0.001, ****P<0.0001; ns, no significance vs the angiotensin II group; ##P<0.01, ###P<0.001 vs the Qβ group. **B**, The ATR-001-specific antibody titer in the vaccine group mice (n>5). **C**, Representative photographs of macroscopic features of aneurysms in each experimental group. **D**, Quantitative analysis of abdominal aortic aneurysm incidence in each experimental group: Control (n=8), angiotensin II (n=23), Telmisartan (n=16), Hydralazine (n=14), Vaccine (n=21), Qβ (n=20). *P<0.0045. **E**, Quantitative analysis of maximal aortic diameter in each experimental group (only of survival mice were included in the diameter statistics): Angiotensin II (n=19), Telmisartan (n=14), Hydralazine (n=13), Vaccine (n=20), Qβ (n=17). *P<0.05, **P<0.01, ***P<0.001. **F**, According to reported classifications, the incidence of advanced abdominal aortic aneurysm was also decreased by the vaccination. Ang II indicates angiotensin II; SBP, systolic blood pressure. *P<0.05, **P<0.01. Data are expressed as means±SEM.

limited by administration of telmisartan or ATRQβ-001 vaccination (Figure 4A). Evidence manifested that ATRQβ-001 and telmisartan also decreased the IL-1β, tumor necrosis factor-α, C-C motif chemokine ligand 2 (CCL2), C-C motif chemokine receptor 2 (CCR2), osteopontin, and AT1R transcription induced by Ang II in aorta tissue (Figure 4B). Interestingly, the impaired peroxisome proliferator-activated receptor γ expression by Ang II was rescued in both
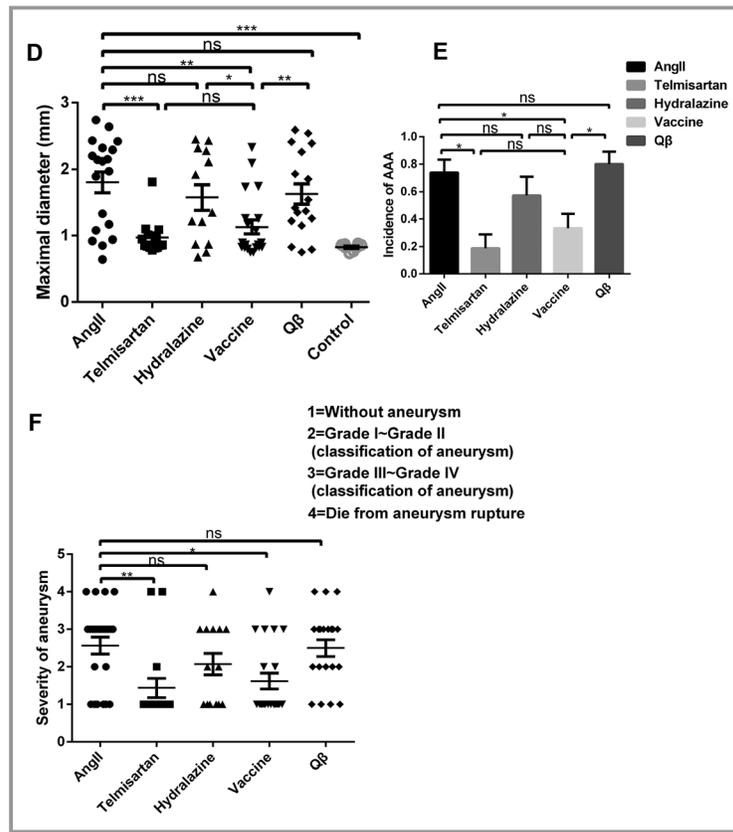
Figure 1. Continued.

telmisartan and vaccine group. Immunohistochemistry demonstrated that persistent Ang II infusion increased osteopontin expression in the media layer, whereas ATRQβ-001 vaccine ameliorated the osteopontin expression (Figure 4C and 4D). ATRQβ-001 vaccine also suppressed CD68-marked macrophages infiltration compared with the Ang II group (Figure 4C and 4E).

Osteopontin (OPN) was recognized as a marker of secretory phenotype of VSMC.[20] Literature reported that VSMC phenotypic modulation played a vital role in early stage of aortic aneurysms,[21,22] we then examined smooth muscle contractile protein in aorta tissue on 7 days post-Ang II perfusion. As expected, expression of VSMC-specific smooth muscle α-actin (α-SMA) and SM22α (transgelin) were notably diminished in the media layer of AAA sections of Ang II group, compared with abdominal aortic sections of saline-treated controls (Figure 5A). Meanwhile, synthetic phenotype markers such as osteopontin and vimentin were slightly increased in the vascular wall (Figure S3). In contrast, additive administration of ATRQβ-001 vaccine or telmisartan redeemed the dedifferentiation of VSMC. Similarly, in vitro experiments revealed that treatment with Ang II significantly increased the transcription of VSMC synthetic phenotype markers vimentin and osteopontin (Figure 5B). However, the

effects were abrogated by pretreatment of telmisartan or monoclonal antibody against the ATR-001 peptide.

As both vimentin and osteopontin were known to foster migration of immune cells,[23,24] we next conducted experiments to investigate the effect of anti-ATR-001 antibody on interaction of Ang II-treated VSMCs with macrophages. In transwell assays, we co-cultured RAW264.7 macrophages with Ang II-treated MOVAS VSMCs and found that the number of macrophages migrated to the underside was dramatically boosted compared with those from RAW264.7 cells co-cultured with PBS-treated MOVAS cells. In contrast, migrated macrophages were pronouncedly attenuated in chambers under RAW264.7 cells co-cultured with anti-ATR-001-pretreated MOVAS cells (Figure 5C and 5D).

ATRQβ-001 Vaccine Suppressed VSMC and Macrophage Derived Proteolysis of extracellular matrix

Dilation of the aorta is typically accompanied by proteolytic disruption of elastin and collagen within the media. Although multiple matrix proteinases are implicated in AAA, there is a predominant focus on MMP-2 and MMP-9.[25,26] Hence, we investigated the effect of ATRQβ-001 vaccine on MMP-2 and
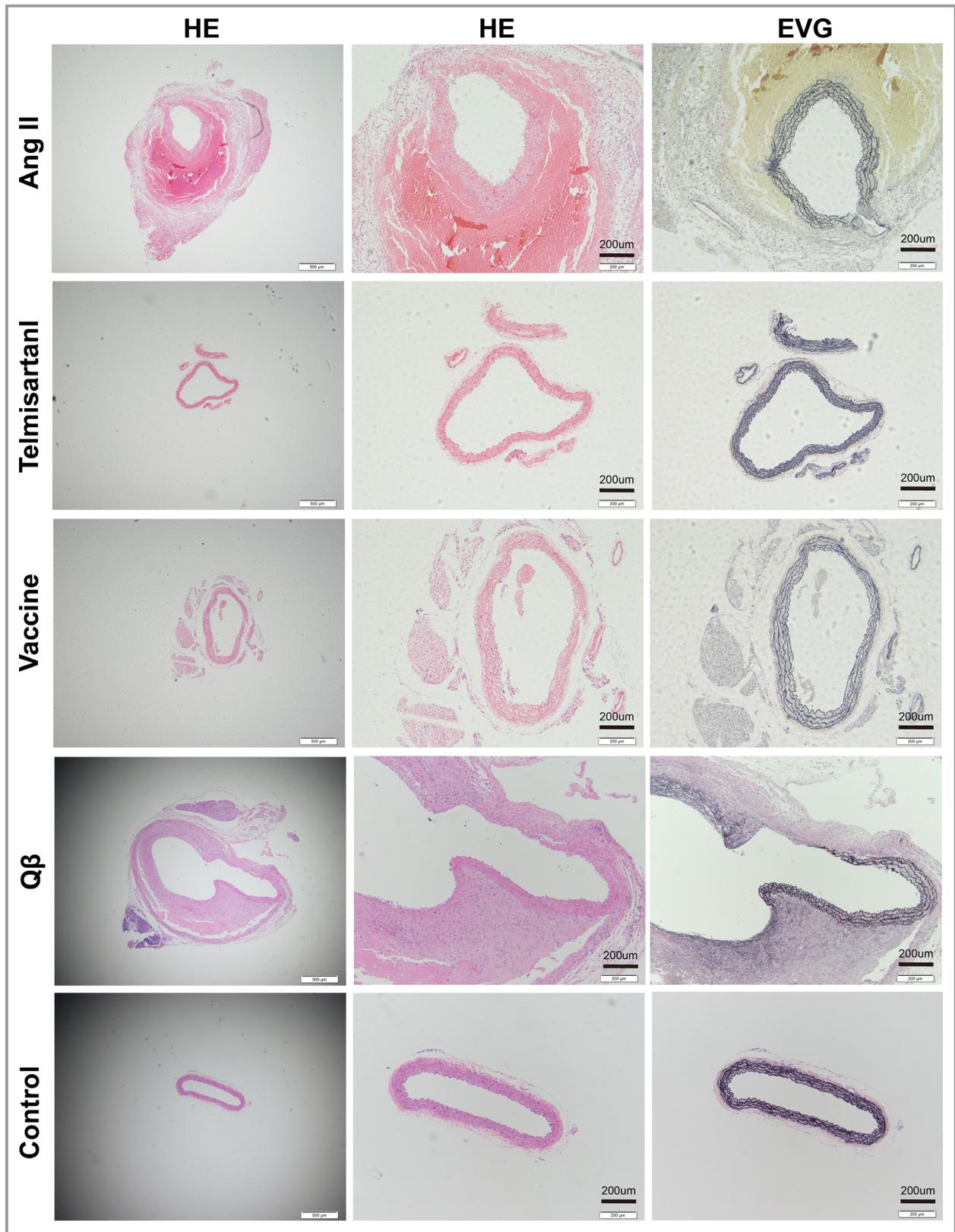
Figure 2. Representative cross-sections of pathological staining. Hematoxylin and eosin staining showed that ATRQβ-001 vaccine effectively prevented the artery dilation and thrombus formation, with the vascular wall relatively intact. Elastic Van Gieson staining showed that ATRQβ-001 vaccine preserved the integrality of medial elastin. Ang II indicates angiotensin II; EVG, Elastic Van Gieson; HE, hematoxylin and eosin. Scale bar represents 200 μm.
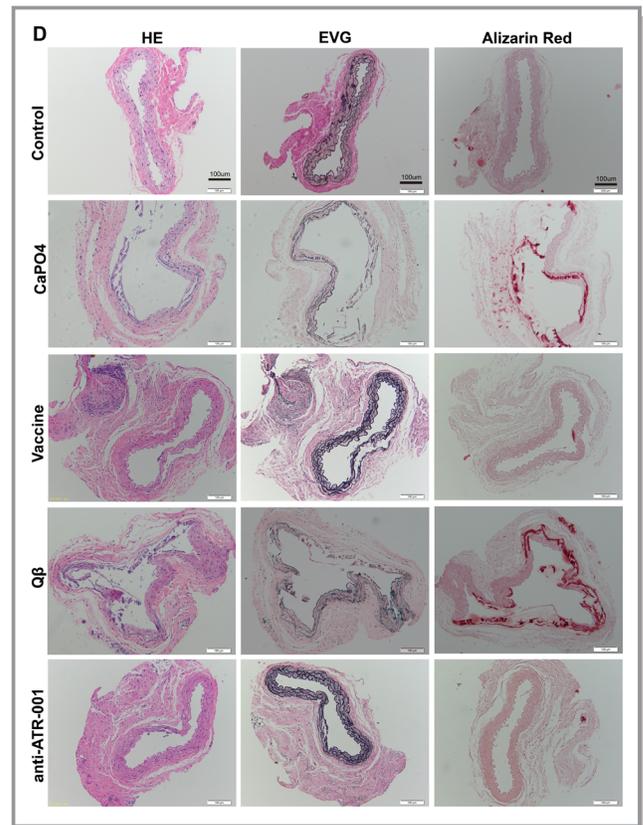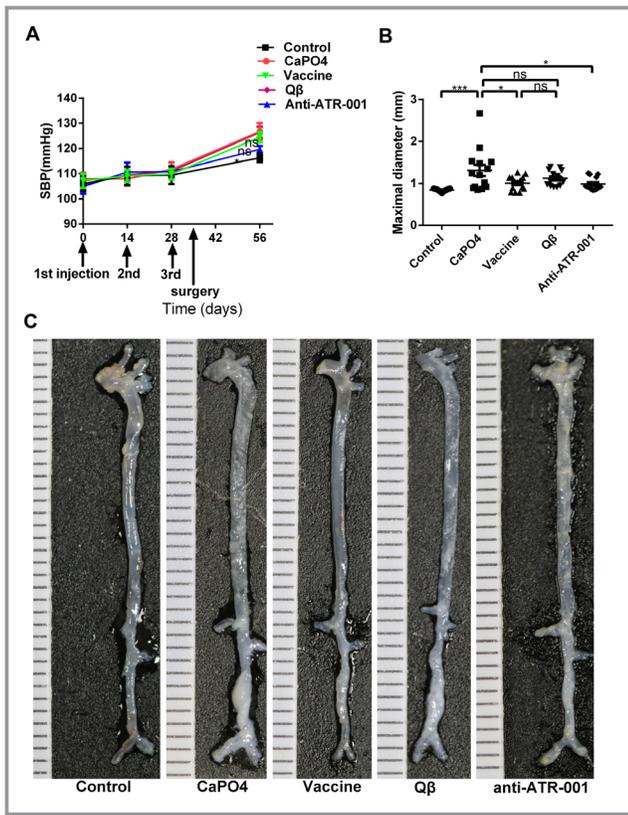
Figure 3. ATRQβ-001 vaccine and anti-ATR-001 antibody prevented aneurysm formation in CaPO₄-induced abdominal aortic aneurysm model. Male C57BL/6 mice were randomized to 5 groups. The vaccine group mice were vaccinated subcutaneously with ATRQβ-001 vaccine ahead of the surgery. The Qβ group were vaccinated with equivalent dosage of Qβ virus-like particle correspondingly. The anti-ATR-001 group mice were injected with anti-ATRQβ-001 monoclonal antibody via caudal veins since the operation. **A**, The systolic blood pressure of C57BL/6 mice (n=5 per group). Data are expressed as means±SEM. *$P<0.05$ vs the CaPO₄ group; ns, no significance vs the CaPO₄ group. **B**, Quantitative analysis of maximal aortic diameter in each experimental group: Control (n=11), CaPO₄ (n=14), Vaccine (n=14), Qβ (n=14), anti-ATR-001 (n=13). Data are expressed as means±SEM. *$P<0.05$, ***$P<0.001$; ns, no significance. **C**, Representative photographs of macroscopic features of aneurysms in each experimental group. **D**, Hematoxylin and eosin staining of representative sections showed the general morphology of vascular wall. Elastic Van Gieson staining showed the elastin integrity in the media. Alizarin Red staining showed the calcification of the media layer. EVG indicates Elastic Van Gieson; HE, hematoxylin and eosin; SBP, systolic blood pressure. Scale bar represents 100 μm.

MMP-9 expression by immunohistochemistry. Ang II significantly elevated the expression of MMP2 and MMP9 as well as the extracellular MMP inducer (EMMPRIN). And the excessive expression of MMP2, MMP9, and EMMPRIN were significantly decreased by ATRQβ-001 vaccination (Figure 6A through 6E). And gelatin zymography showed that the activity of MMP2 and MMP9 was retrained by ATRQβ-001

Figure 3. Continued.

vaccine (Figure 6F). Quantitative real-time polymerase chain reaction of aorta tissues also manifested that ATRQβ-001 vaccine diminished the transcription of MMP2 and MMP9, compared with the Ang II group (Figure 6G). In human AAA tissue, MMP-2 is mainly expressed by resident mesenchymal cells[27] while MMP-9 is primarily derived from macrophage.[28] Thus we further investigated the effect of anti-ATR-001 on proteolytic matrix proteinases secreted from VSMC and macrophage in vitro. Consistent with in vivo experiments, Ang II significantly induced the transcription of MMP2 and EMMPRIN in MOVAS cells (Figure 6H) as well as MMP9 and cathepsins in RAW264.7 macrophages (Figure 6I). But the effects were obviously decreased when cells were pretreated with anti-ATR-001 antibody. In addition, we treated RAW264.7 cells with LPS and found that anti- ATR-001 antibody also decreased lipopolysaccharide (LPS)-induced MMPs expression (Figure S4).

Anti–ATRQβ-001 Antibody Specifically Bound to AT1R and Effectively Inhibited Activation of AngII-AT1R Signaling Transduction

As the ATRQβ-001 peptide was derived from the second extracellular loop of human AT1R, we used immunofluorescence to confirm the ability of anti–ATR-001 antibody to detect
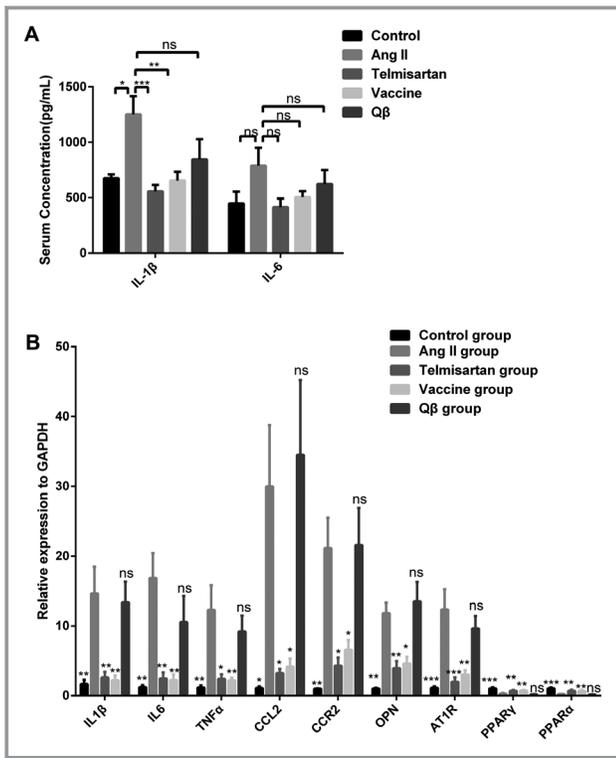
Figure 4. ATRQβ-001 vaccine alleviated vascular inflammation induced by angiotensin II. **A**, Serum concentration of interleukin-1β and -6 were detected by ELISA kit (n=4–10 per group). **B**, The levels of proinflammatory factor, peroxisome proliferator-activated receptor-α and -γ mRNA expression in aorta tissues were measured by quantitative real-time polymerase chain reaction (n>4 per group). *$P<0.05$, **$P<0.01$, ***$P<0.001$; ns, no significance vs the angiotensin II group. **C**, Representative histochemistry staining sections of osteopontin and CD68. Scale bar represents 500 μm (white) in low-power field and 100 μm (red) in high-power field. **D**, Quantitative analysis of osteopontin expression in abdominal aortic aneurysm sections (n>4 per group). **E**, Quantitative analysis of CD68 expression in abdominal aortic aneurysm sections (n>4 per group). **A**, **C** through **E**, *$P<0.05$, **$P<0.01$, ***$P<0.001$; ns, no significance. All the data are expressed as means±SEM. Ang indicates angiotensin II; AT1R, angiotensin II receptor type 1; CCL2, C-C motif chemokine ligand 2; CCR2 C-C motif chemokine receptor 2; IL-1β, interleukin-1β; IL-6, interleukin-6; OPN, osteopontin; PPARα, peroxisome proliferator-activated receptor α; PPARγ, peroxisome proliferator-activated receptor γ; TNFα, tumor necrosis factor α.

the AT1R protein. After treating with Ang II for 24 hours, the CHO-K1 cells transfected with human AT1R plasmid were fixed. Commercial anti-AT1R antibody (Abcam) effectively bonded to the cytomembrane and fluorescence was detected when cells climbing were incubated with appropriate fluorescent antibody. When fixed cells climbing were incubated with mouse-derived anti–ATR-001 antibody and anti-mouse fluorescent antibody, fluorescence can also be detected on the cytomembrane (Figure 7A). In contrast, normal mouse immunoglobulin G failed to bond to the Ang II-treated-CHO-AT1R cells climbing. Besides,
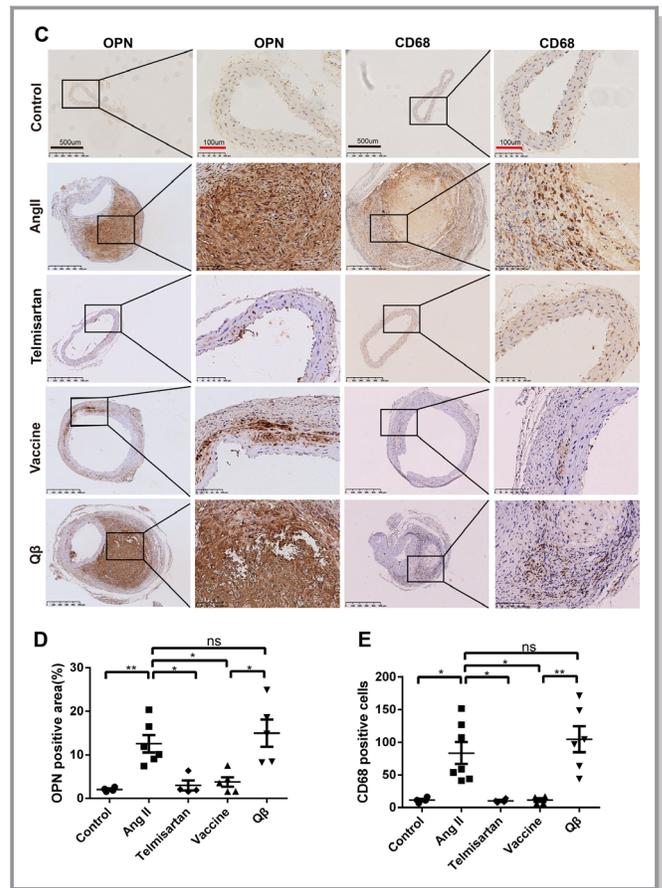
Figure 4. Continued.

we examined the effect of anti–ATR-001 antibody on AT1R expression in MOVAS cells. Results demonstrated that Ang II-induced AT1R expression was decreased when pretreated with anti–ATR-001 antibody (Figure 7B), contrast to normal mouse immunoglobulin G.

Discussion

In the present study, we demonstrated for the first time that the vaccination with ATRQβ-001 vaccine effectively impeded the formation and progression of AAA under circumstance of 2 different animal models.

Piles of literatures have testified that Ang II-induced AAAs recapitulate many pathological features of human AAAs (or more accurately defined as dissecting AAA[29–31]). These include male preponderance, often atherosclerosis accompanied, medial elastin fiber destruction, collagen degradation and maladaptive deposition, intramural thrombus formation, inflammatory cell accumulation, aortic dissection and rupture.[32,33] All these features highlighted the effects of the endogenous activation of Ang II in AAA pathogenesis. In the meantime, Ang II and Ang II-forming enzymes were found to
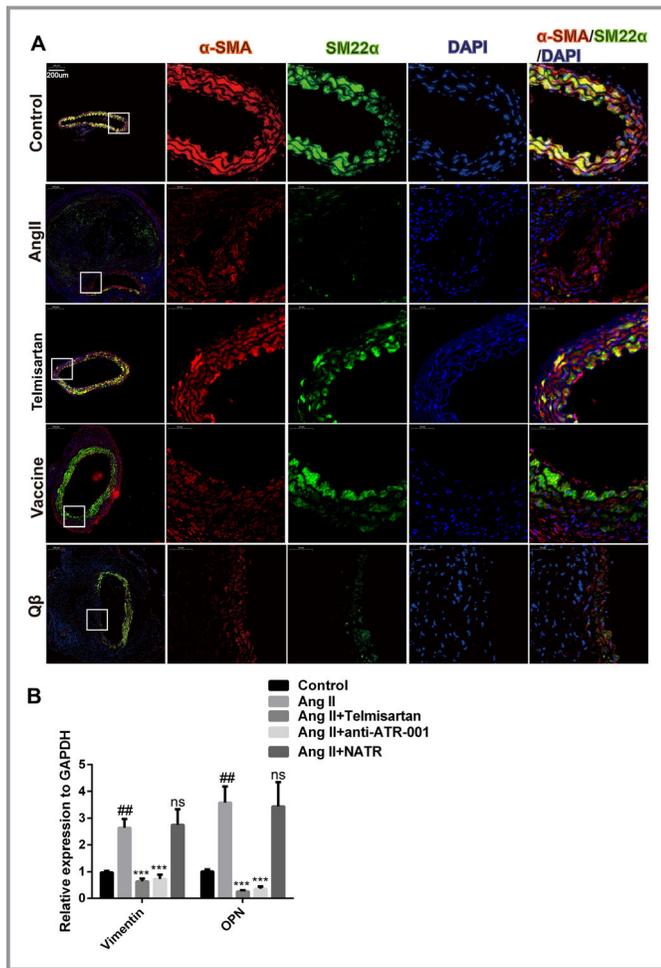
Figure 5. ATRQβ-001 vaccine prevented vascular smooth muscle cell phenotypic transition. **A,** Expression of sections of α-SMA (red) and SM22α (green) on abdominal aorta sections on 7 days post angiotensin II infusion were detected by immunofluorescence. Scale bar represents 200 μm. **B,** The anti-ATR-001 antibody inhibited synthetic phenotype markers transcription in vascular smooth muscle cell. Mouse aorta vascular smooth cell line cells were pretreated with the anti-ATR-001 antibody (10 μg/mL), telmisartan (1×10^{-6} mol/L), or normal mouse immunoglobulin G for 2 hours, respectively, and then incubated with angiotensin II (1×10^{-5} mol/L) for 72 hours. The relative mRNA expression of vimentin and osteopontin in vascular smooth muscle cells were detected by quantitative real-time polymerase chain reaction. ***$P<0.001$ vs the angiotensin II group; ##$P<0.01$ vs the control group. **C,** Osteopontin produced by vascular smooth muscle cell recruited macrophages. Mouse aorta vascular smooth cell line cells were pretreated with the anti-ATR-001 antibody (10 μg/mL), telmisartan (1×10^{-6} mol/L), or normal mouse immunoglobulin G for 2 hours, respectively, subsequently stimulated by angiotensin II (1×10^{-5} mol/L) for 72 hours before co-cultured with RAW264.7 cells for another 12 hours. The migration of macrophages toward vascular smooth muscle cells was measured by transwell chamber migration assay. High-power field ×100). **D,** Quantitative analysis of macrophage number migrated to the underside. **$P<0.01$, ****$P<0.0001$. All the data are expressed as means±SEM of 3 independent experiments. Ang II indicates angiotensin II; MOVAS, mouse aorta vascular smooth muscle cell line; NATR, normal mouse immunoglobulin G; RAW264.7, mouse macrophage cell line.
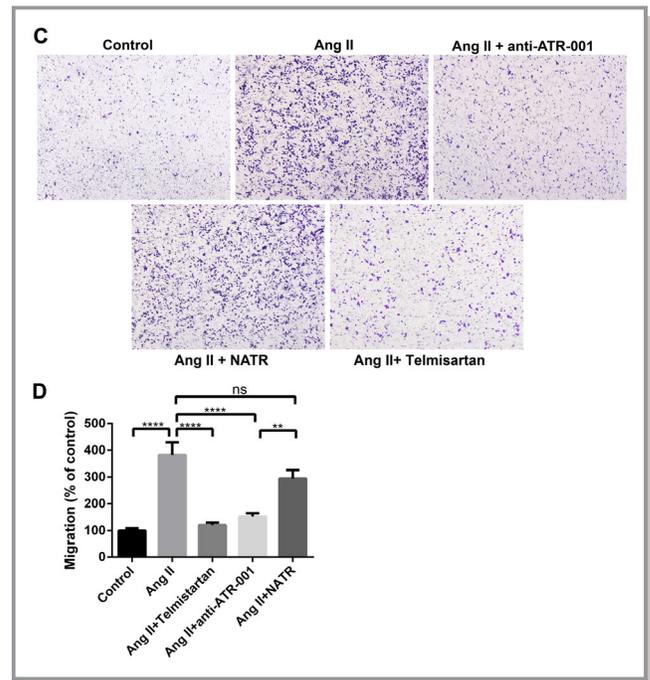
Figure 5. Continued.

be upregulated in human aneurysm.[9–11] Thus, we focused on the Ang II-ApoE$^{-/-}$ AAA model to illustrate the activities of ATRQβ-001 vaccine on AAA and the mechanisms beneath.

In the Ang II-induced AAA model, ATRQβ-001 vaccine inhibited the blood pressure elevation and AAA formation compared with the Ang II group, resembling to the effect of telmisartan. Although hydralazine successfully decreased the blood pressure, the incidence of AAA and maximal aortic diameter didn't show statistical significance with the Ang II group. These indicated that reduction of blood pressure did not afford protection against AAA formation and progression. In the meantime, Qβ VLP vaccination failed to prevent neither the elevation of blood pressure nor formation of aneurysm, implying the specific competence of the ATRQβ-001 peptide. What's noteworthy is that the ATRQβ-001 vaccine had minimal impacts on normal blood pressure although animals were given 3 injections ahead of Ang II administration, which implied the possibility to securely take precautions against AAA without affecting normal basal systolic blood pressure. The effects of ATRQβ-001 vaccine and specific anti-ATR-001 antibody were confirmed in another AAA animal model induced by CaCl$_2$/PBS (the CaPO$_4$-induced AAA model). Although ATRQβ-001 vaccine and anti-ATR-001 antibody didn't decrease the systolic blood pressure significantly in CaPO$_4$-induced AAA model, the aorta dilation and elastin fraction were obviously ameliorated.

Since chronic inflammation in the aortic wall and loss of medial VSMCs feature the pathological damage of AAA, we first examined the effect of ATRQβ-001 vaccine on
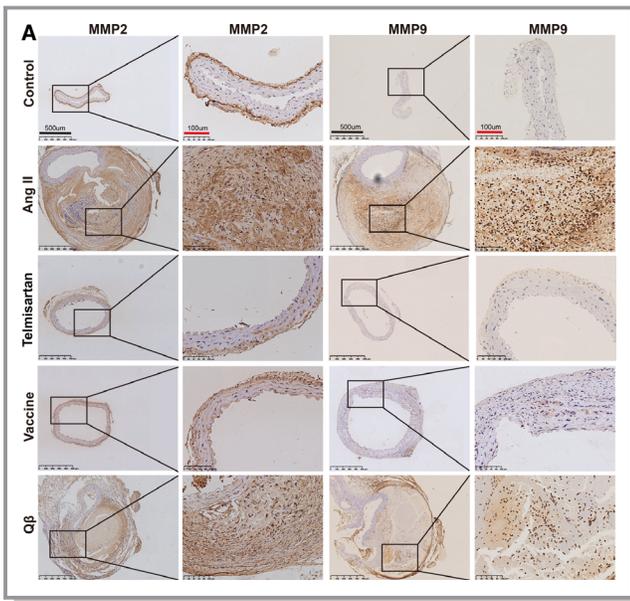
Figure 6. ATRQβ-001 vaccine and anti-ATR-001 antibody suppressed proteolysis of extracellular matrix (ECM). **A,** Representative histochemistry staining sections of matrix metalloproteinase (MMP)2 and MMP9. Scale bar represents 500 μm in low-power field and 100 μm in high-power field. **B,** Quantitative analysis of MMP2 expression in abdominal aortic aneurysm sections (n>4 per group). ***P<0.001, ****P<0.0001. **C,** Quantitative analysis of MMP2 expression in abdominal aortic aneurysm sections (n>4 per group). *P<0.05, **P<0.01, ***P<0.001. **D,** Representative histochemistry staining sections of extracellular MMP inducer. Scale bar represents 500 μm (white) in low-power field and 100 μm (red) in high-power field. **E,** Quantitative analysis of extracellular MMP inducer expression in abdominal aortic aneurysm sections (n>4 per group). *P<0.05, **P<0.01. **F,** Gelatin zymography to detect activities of MMP-2 and MMP-9 in aortas. **G,** The levels of matrix associated proteins transcription in aorta tissues were measured by quantitative real-time polymerase chain reaction (n>5 per group). *P<0.05, **P<0.01, ***P<0.001, ****P<0.0001 vs the angiotensin II group. **H,** Mouse aorta vascular smooth cell line cells were pretreated with the anti-ATR-001 antibody (10 μg/mL), telmisartan (1×10^{-6} mol/L), or normal mouse immunoglobulin G (NATR) for 2 hours, respectively, subsequently stimulated by angiotensin II (1×10^{-5} mol/L) for 72 hours. The levels of MMP2 and extracellular MMP inducer mRNA expression in vascular smooth muscle cell were measured by quantitative real-time polymerase chain reaction. **I,** RAW264.7 cells were pretreated with the anti-ATR-001 antibody (10 μg/mL), telmisartan (1×10^{-6} mol/L), or normal mouse immunoglobulin G (NATR) for 2 hours, respectively, subsequently stimulated by angiotensin II (1×10^{-5} mol/L) for 24 hours. The levels of MMP9 and cathepsins mRNA expression in macrophages were measured by quantitative real-time polymerase chain reaction. **H** and **I,** *P<0.05, **P<0.01, ***P<0.001 vs the angiotensin II group; #P<0.05, ###P<0.001 vs the control group. All the data are expressed as means±SEM of 3 independent experiments. Ang II indicates angiotensin II; CTSK, cathepsin K; CTSL, cathepsin L; CTSS, cathepsin S; EMMPRIN, extracellular MMP inducer; MMP, matrix metalloproteinase; MOVAS, mouse aorta vascular smooth cell line; NATR, normal mouse immunoglobulin G; RAW264.7, mouse macrophage cell line; TIMP-1, tissue inhibitors of metalloproteinase 1.
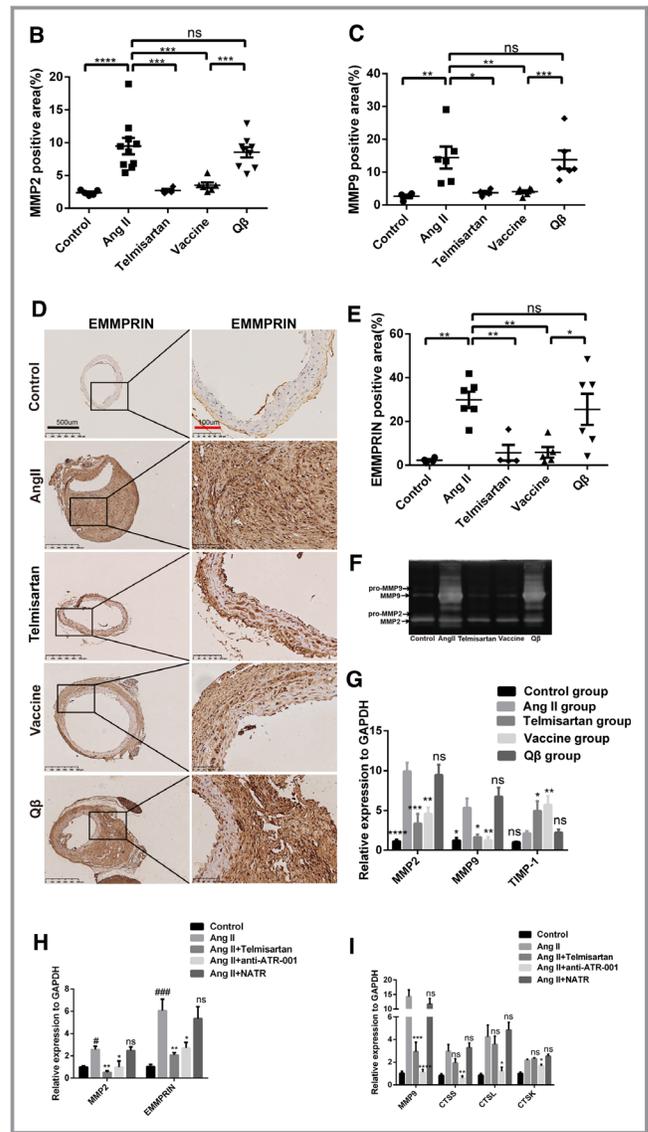
Figure 6. Continued.

inflammatory response. Evidence demonstrated that ATRQβ-001 vaccine ameliorated Ang II–induced inflammatory cytokines in plasma and in the aorta tissue. Osteopontin is reported to promote the adhesion, migration, and activation of macrophages.[34–36] Meanwhile, it is one of the secretory phenotype markers in VSMC and participate in VSMC dedifferentiation.[20,37] In vivo and vitro experiments demonstrated that ATRQβ-001 vaccine and anti-ATR-001 antibody inhibited the transformation of VSMC from contractile phenotype to synthetic phenotype, attenuated osteopontin and vimentin expression in VSMC. In transwell assays, the migration of macrophage induced by coculture with Ang II–treated VSMC was suppressed by the anti-ATR-001 antibody, which corresponded with the findings of decreased macrophage (marked by CD68) infiltration in the aneurysm section.
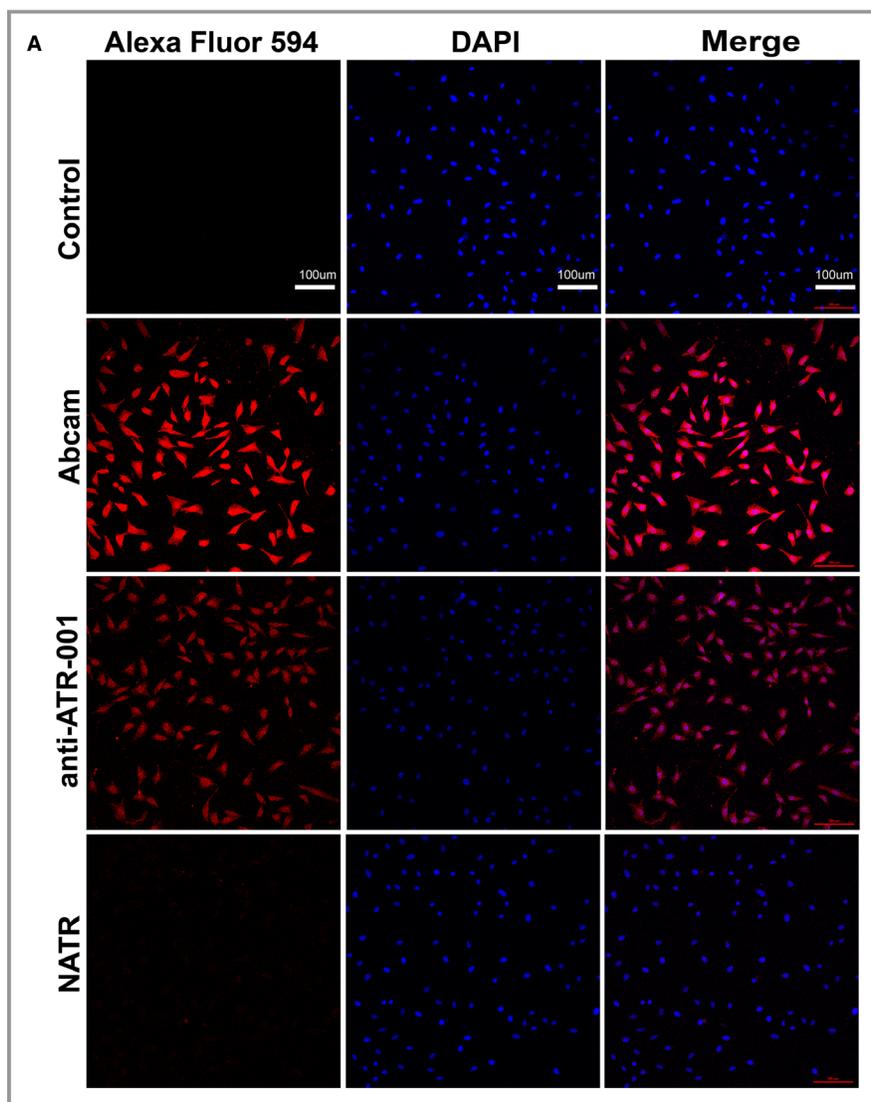
Figure 7. Anti–ATRQβ-001 antibody specifically bound to angiotensin II type 1 receptor and effectively Inhibited activation of angiotensin II type 1 receptor activation. **A**, CHO-K1 cells were stably transfected with angiotensin II type 1 receptor. The binding ability of anti-ATR-001 antibody to angiotensin II type 1 receptor was detected by immunofluorescence. Cell nucleus were stained by 4′,6-diamidino-2-phenylindole (DAPI). Scale bar represents 100 μm. **B**, Mouse aorta vascular smooth cell line cells were pretreated with the anti-ATR-001 antibody (10 μg/mL), telmisartan (1×10^{-6} mol/L), or normal mouse immunoglobulin G for 2 hours, respectively, subsequently stimulated by angiotensin II (1×10^{-5} mol/L) for 72 hours. The level of angiotensin II type 1 receptor was measured by western blot. All the data are expressed as means±SEM of 3 independent experiments. *$P<0.05$, **$P<0.01$, ***$P<0.001$ vs the angiotensin II group. Ang II indicates angiotensin II; AT1R, angiotensin II type 1 receptor; MOVAS, mouse aorta vascular smooth cell line; NATR, normal mouse immunoglobulin G.

As dilation of the aorta is typically accompanied by proteolytic degradation of extracellular matrix, we subsequently examined effects of ATRQβ-001 vaccine and anti- ATR-001 antibody on proteolytic matrix proteinases. Results indicated that anti-ATR001 effectively lowered MMPs and cathepsins in macrophages as well as the MMP2 and extracellular MMP inducer (EMMPRIN) in VSMCs.

We had elaborated in different animal models that no immune-mediated damages and few feedbacked activation of circulating or local renin–angiotensin-aldosterone system was found in the vaccinated animals, while the plasma renin activity and concentration of Ang II were significantly increased in mice administrated with valsartan or olmesartan.[12–14] Direct inhibition of renin activity using aliskiren was
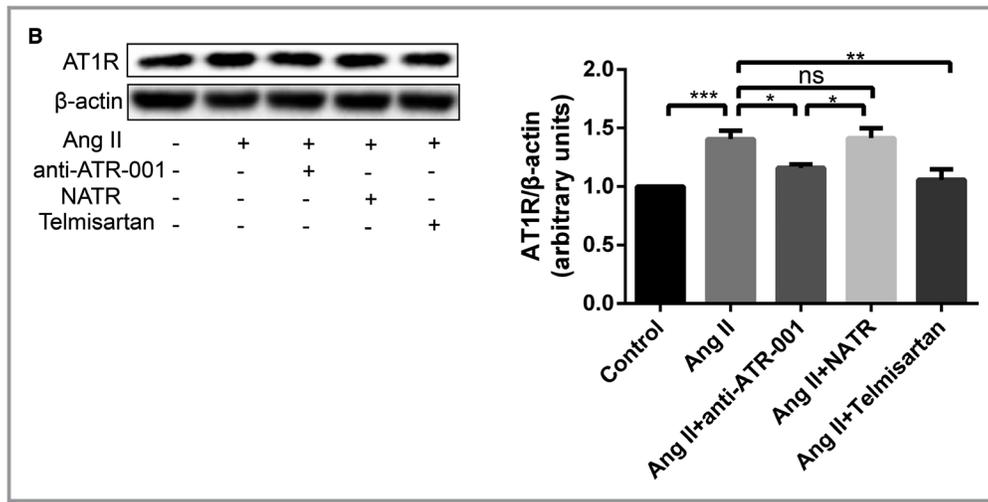
Figure 7. Continued.

demonstrated to prevent the progression of aortic aneurysm,[38] which means that the feedbacked augment of renin activity may cripple the therapeutic efficiency of angiotensin II receptor type-1 blocker. These partially explained the controversial conclusions of angiotensin II receptor type-1 blocker used in experimental AAA studies.[17,39–41] Telmisartan, with its unique structure resembling to pioglitazone, was proved to inhibit AAAs in several different animal models.[8,42–44] We assume that it may be the synergy of AT1R inhibition and peroxisome proliferator-activated receptor γ activation which contribute to the protective effect. In the present study, apart from AT1R inhibition, vaccination of the ATRQβ-001 vaccine also elevated peroxisome proliferator-activated receptor γ expression, which indicated the comparability of the ATRQβ-001 vaccine to telmisartan. Notably, the dose of telmisartan used to prevent experimental aortic aneurysm was 5 mg/kg per day in our study or 10 mg/kg/d in most studies, which was much larger than the clinical usage. Thus, the therapeutic effect of telmisartan in clinical application remains doubtful. The TEDY (Telmisartan in the Management of Abdominal Aortic Aneurysm) trial, a multicenter randomized controlled trial, is currently undergoing to test the efficacy of telmisartan 40 mg/day in suppressing early AAA disease progression,[45] and the final result is unknown to date.

We had previously reported the beneficial effect of ATRQβ-001 vaccine on hypertension, diabetic nephropathy as well as atherosclerosis.[12–14] ATRQβ-001 vaccination suppressed Ang II-AT1R activation and pathological signal pathway overactivity, protecting hypertension associated target organs. The current findings took a step forward to confirm the efficacy of ATRQβ-001 vaccine on aneurysm prevention. Although the anti-hypertensive effect of ATRQβ-001 vaccine was weaker than angiotensin II receptor type-1 blocker, it remained efficient to retard the pathological progress of AAA.

Considering the half-life of the specific vaccine antibody,[12] 14.4 days, much longer than any other chemical drugs presently used, approaches of vaccination manifested superior advantages to improve compliance of patients.

However, there are some limitations in our study. On one hand, compared with the apoB-100–related peptide vaccine,[46] we need larger sample capacity to assess the mortality to confirm the effect of ATRQβ-001 vaccine on AAA mortality. On the other hand, clinical data are needed to authenticate the effectiveness of the vaccine, since there are no ideal animal models that completely recapitulate all characteristics yet and conclusions from experimental animal AAA and human AAA are often discrepant.

Conclusions

In summary, we demonstrated for the first time that ATRQβ-001 vaccine effectively inhibited the incidence and progression of AAA in different experimental AAA models. Immunization of the ATRQβ-001 vaccine minimized administration frequency and didn't affect normal blood pressure, may serve as a promising preventative avenue to aneurysm.

Sources of Funding

Disclosures

None.

References

1. Rajiah P, Reiber JH, Partovi S. Population based ultrasonographic screening of abdominal aortic aneurysms. *Int J Cardiovasc Imaging*. 2016;32:1605–1607.

2. Choke E, Vijaynagar B, Thompson J, Nasim A, Bown MJ, Sayers RD. Changing epidemiology of abdominal aortic aneurysms in England and Wales: older and more benign? *Circulation*. 2012;125:1617–1625.

3. Brewster DC, Cronenwett JL, Hallett JW Jr, Johnston KW, Krupski WC, Matsumura JS; Joint Council of the American Association for Vascular Surgery and Society for Vascular Surgery. Guidelines for the treatment of abdominal aortic aneurysms. Report of a subcommittee of the Joint Council of the American Association for Vascular Surgery and Society for Vascular Surgery. *J Vasc Surg*. 2003;37:1106–1117.

4. Mortality results for randomised controlled trial of early elective surgery or ultrasonographic surveillance for small abdominal aortic aneurysms. The UK Small Aneurysm Trial Participants. *Lancet*. 1998;352:1649–1655.

5. Lederle FA, Wilson SE, Johnson GR, Reinke DB, Littooy FN, Acher CW, Ballard DJ, Messina LM, Gordon IL, Chute EP, Krupski WC, Busuttil SJ, Barone GW, Sparks S, Graham LM, Rapp JH, Makaroun MS, Moneta GL, Cambria RA, Makhoul RG, Eton D, Ansel HJ, Freischlag JA, Bandyk D; Aneurysm Detection and Management Veterans Affairs Cooperative Study Group. Immediate repair compared with surveillance of small abdominal aortic aneurysms. *N Engl J Med*. 2002;346:1437–1444.

6. Chaikof EL, Dalman RL, Eskandari MK, Jackson BM, Lee WA, Mansour MA, Mastracci TM, Mell M, Murad MH, Nguyen LL, Oderich GS, Patel MS, Schermerhorn ML, Starnes BW. The Society for Vascular Surgery practice guidelines on the care of patients with an abdominal aortic aneurysm. *J Vasc Surg*. 2018;67:2.

7. Cassis LA, Rateri DL, Lu H, Daugherty A. Bone marrow transplantation reveals that recipient AT1a receptors are required to initiate angiotensin II-induced atherosclerosis and aneurysms. *Arterioscler Thromb Vasc Biol*. 2007;27:380–386.

8. Xuan H, Xu B, Wang W, Tanaka H, Fujimura N, Miyata M, Michie SA, Dalman RL. Inhibition or deletion of angiotensin II type 1 receptor suppresses elastase-induced experimental abdominal aortic aneurysms. *J Vasc Surg*. 2018;67:573–584.e572.

9. Ihara M, Urata H, Kinoshita A, Suzumiya J, Sasaguri M, Kikuchi M, Ideishi M, Arakawa K. Increased chymase-dependent angiotensin II formation in human atherosclerotic aorta. *Hypertension*. 1999;33:1399–1405.

10. Nishimoto M, Takai S, Fukumoto H, Tsunemi K, Yuda A, Sawada Y, Yamada M, Jin D, Sakaguchi M, Nishimoto Y, Sasaki S, Miyazaki M. Increased local angiotensin II formation in aneurysmal aorta. *Life Sci*. 2002;71:2195–2205.

11. Tsunemi K, Takai S, Nishimoto M, Yuda A, Hasegawa S, Sawada Y, Fukumoto H, Sasaki S, Miyazaki M. Possible roles of angiotensin II-forming enzymes, angiotensin converting enzyme and chymase-like enzyme, in the human aneurysmal aorta. *Hypertens Res*. 2002;25:817–822.

12. Chen X, Qiu Z, Yang S, Ding D, Chen F, Zhou Y, Wang M, Lin J, Yu X, Zhou Z, Liao Y. Effectiveness and safety of a therapeutic vaccine against angiotensin II receptor type 1 in hypertensive animals. *Hypertension*. 2013;61:408–416.

13. Ding D, Du Y, Qiu Z, Yan S, Chen F, Wang M, Yang S, Zhou Y, Hu X, Deng Y, Wang S, Wang L, Zhang H, Wu H, Yu X, Zhou Z, Liao Y, Chen X. Vaccination against type 1 angiotensin receptor prevents streptozotocin-induced diabetic nephropathy. *J Mol Med (Berl)*. 2016;94:207–218.

14. Zhou Y, Wang S, Qiu Z, Song X, Pan Y, Hu X, Zhang H, Deng Y, Ding D, Wu H, Yang S, Wang M, Zhou Z, Liao Y, Chen X. ATRQbeta-001 vaccine prevents atherosclerosis in apolipoprotein E-null mice. *J Hypertens*. 2016;34:474–485; discussion 485.

15. Lu H, Howatt DA, Balakrishnan A, Moorleghen JJ, Rateri DL, Cassis LA, Daugherty A. Subcutaneous angiotensin II infusion using osmotic pumps induces aortic aneurysms in mice. *J Vis Exp*. 2015;103. DOI: 10.3791/53191.

16. Yamanouchi D, Morgan S, Stair C, Seedial S, Lengfeld J, Kent KC, Liu B. Accelerated aneurysmal dilation associated with apoptosis and inflammation in a newly developed calcium phosphate rodent abdominal aortic aneurysm model. *J Vasc Surg*. 2012;56:455–461.

17. Daugherty A, Manning MW, Cassis LA. Antagonism of AT2 receptors augments angiotensin II-induced abdominal aortic aneurysms and atherosclerosis. *Br J Pharmacol*. 2001;134:865–870.

18. Manning MW, Cassi LA, Huang J, Szilvassy SJ, Daugherty A. Abdominal aortic aneurysms: fresh insights from a novel animal model of the disease. *Vasc Med*. 2002;7:45–54.

19. Poulsen JL, Stubbe J, Lindholt JS. Animal models used to explore abdominal aortic aneurysms: a systematic review. *Eur J Vasc Endovasc Surg*. 2016;52:487–499.

20. Giachelli CM, Speer MY, Li X, Rajachar RM, Yang H. Regulation of vascular calcification: roles of phosphate and osteopontin. *Circ Res*. 2005;96:717–722.

21. Ailawadi G, Moehle CW, Pei H, Walton SP, Yang Z, Kron IL, Lau CL, Owens GK. Smooth muscle phenotypic modulation is an early event in aortic aneurysms. *J Thorac Cardiovasc Surg*. 2009;138:1392–1399.

22. Salmon M, Johnston WF, Woo A, Pope NH, Su G, Upchurch GR Jr, Owens GK, Ailawadi G. KLF4 regulates abdominal aortic aneurysm morphology and deletion attenuates aneurysm formation. *Circulation*. 2013;128:S163–S174.

23. Nieminen M, Henttinen T, Merinen M, Marttila-Ichihara F, Eriksson JE, Jalkanen S. Vimentin function in lymphocyte adhesion and transcellular migration. *Nat Cell Biol*. 2006;8:156–162.

24. Weber GF, Zawaideh S, Hikita S, Kumar VA, Cantor H, Ashkar S. Phospho-rylation-dependent interaction of osteopontin with its receptors regulates macrophage migration and activation. *J Leukoc Biol*. 2002;72:752–761.

25. Thompson RW, Parks WC. Role of matrix metalloproteinases in abdominal aortic aneurysms. *Ann N Y Acad Sci*. 1996;800:157–174.

26. Longo GM, Xiong W, Greiner TC, Zhao Y, Fiotti N, Baxter BT. Matrix metalloproteinases 2 and 9 work in concert to produce aortic aneurysms. *J Clin Invest*. 2002;110:625–632.

27. Davis V, Persidskaia R, Baca-Regen L, Itoh Y, Nagase H, Persidsky Y, Ghorpade A, Baxter BT. Matrix metalloproteinase-2 production and its binding to the matrix are increased in abdominal aortic aneurysms. *Arterioscler Thromb Vasc Biol*. 1998;18:1625–1633.

28. Hibbs MS. Expression of 92 kDa phagocyte gelatinase by inflammatory and connective tissue cells. *Matrix Suppl*. 1992;1:51–57.

29. Trachet B, Fraga-Silva RA, Piersigilli A, Tedgui A, Sordet-Dessimoz J, Astolfo A, Van der Donckt C, Modregger P, Stampanoni MF, Segers P, Stergiopulos N. Dissecting abdominal aortic aneurysm in Ang II-infused mice: suprarenal branch ruptures and apparent luminal dilatation. *Cardiovasc Res*. 2015;105:213–222.

30. Trachet B, Aslanidou L, Piersigilli A, Fraga-Silva RA, Sordet-Dessimoz J, Villanueva-Perez P, Stampanoni MFM, Stergiopulos N, Segers P. Angiotensin II infusion into ApoE(-/-) mice: a model for aortic dissection rather than abdominal aortic aneurysm? *Cardiovasc Res*. 2017;113:1230–1242.

31. Senemaud J, Caligiuri G, Etienne H, Delbosc S, Michel JB, Coscas R. Translational relevance and recent advances of animal models of abdominal aortic aneurysm. *Arterioscler Thromb Vasc Biol*. 2017;37:401–410.

32. Michel JB, Martin-Ventura JL, Egido J, Sakalihasan N, Treska V, Lindholt J, Allaire E, Thorsteinsdottir U, Cockerill G, Swedenborg J; Consortium FE. Novel aspects of the pathogenesis of aneurysms of the abdominal aorta in humans. *Cardiovasc Res*. 2011;90:18–27.

33. Bruemmer D, Daugherty A, Lu H, Rateri DL. Relevance of angiotensin II-induced aortic pathologies in mice to human aortic aneurysms. *Ann N Y Acad Sci*. 2011;1245:7–10.

34. Giachelli CM, Lombardi D, Johnson RJ, Murry CE, Almeida M. Evidence for a role of osteopontin in macrophage infiltration in response to pathological stimuli in vivo. *Am J Pathol*. 1998;152:353–358.

35. Giachelli CM, Steitz S. Osteopontin: a versatile regulator of inflammation and biomineralization. *Matrix Biol*. 2000;19:615–622.

36. Scatena M, Liaw L, Giachelli CM. Osteopontin: a multifunctional molecule regulating chronic inflammation and vascular disease. *Arterioscler Thromb Vasc Biol*. 2007;27:2302–2309.

37. Gao H, Steffen MC, Ramos KS. Osteopontin regulates alpha-smooth muscle actin and calponin in vascular smooth muscle cells. *Cell Biol Int*. 2012;36:155–161.

38. Miyake T, Miyake T, Shimizu H, Morishita R. Inhibition of aneurysm progression by direct renin inhibition in a rabbit model. *Hypertension*. 2017;70:1201–1209.

39. Liao S, Miralles M, Kelley BJ, Curci JA, Borhani M, Thompson RW. Suppression of experimental abdominal aortic aneurysms in the rat by treatment with angiotensin-converting enzyme inhibitors. *J Vasc Surg*. 2001;33:1057–1064.

40. Nagashima H, Uto K, Sakomura Y, Aoka Y, Sakuta A, Aomi S, Hagiwara N, Kawana M, Kasanuki H. An angiotensin-converting enzyme inhibitor, not an angiotensin II type-1 receptor blocker, prevents beta-aminopropionitrile monofumarate-induced aortic dissection in rats. *J Vasc Surg*. 2002;36:818–823.

41. Fujiwara Y, Shiraya S, Miyake T, Yamakawa S, Aoki M, Makino H, Nishimura M, Morishita R. Inhibition of experimental abdominal aortic aneurysm in a rat model by the angiotensin receptor blocker valsartan. *Int J Mol Med*. 2008;22:703–708.

42. Kaschina E, Schrader F, Sommerfeld M, Kemnitz UR, Grzesiak A, Krikov M, Unger T. Telmisartan prevents aneurysm progression in the rat by inhibiting proteolysis, apoptosis and inflammation. *J Hypertens*. 2008;26:2361–2373.

43. Matsumoto S, Kamide K, Banno F, Inoue N, Mochizuki N, Kawano Y, Miyata T. Impact of RGS2 deficiency on the therapeutic effect of telmisartan in angiotensin II-induced aortic aneurysm. *Hypertens Res*. 2010;33:1244–1249.

ORIGINAL RESEARCH

44. Iida Y, Xu B, Schultz GM, Chow V, White JJ, Sulaimon S, Hezi-Yamit A, Peterson SR, Dalman RL. Efficacy and mechanism of angiotensin II receptor blocker treatment in experimental abdominal aortic aneurysms. *PLoS One*. 2012;7:e49642.

45. Morris DR, Cunningham MA, Ahimastos AA, Kingwell BA, Pappas E, Bourke M, Reid CM, Stijnen T, Dalman RL, Aalami OO, Lindeman JH, Norman PE, Walker PJ, Fitridge R, Bourke B, Dear AE, Pinchbeck J, Jaeggi R, Golledge J. Telmisartan in the management of abdominal aortic aneurysm (TEDY): the study protocol for a randomized controlled trial. *Trials*. 2015;16:274.

46. Honjo T, Chyu KY, Dimayuga PC, Yano J, Lio WM, Trinidad P, Zhao X, Zhou J, Chen S, Cercek B, Arditi M, Shah PK. ApoB-100-related peptide vaccine protects against angiotensin II-induced aortic aneurysm formation and rupture. *J Am Coll Cardiol*. 2015;65:546–556.

Supplemental Material

Table S1. Primers sequence for quantitative real-time PCR.

Molecules		Sequence(5'-3')
GAPDH	forward	GCAGTGGCAAAGTGGAGATT
	reverse	CGCTCCTGGAAGATGGTGAT
TNFα	forward	CCCCTTTATTGTCTACTCCTCA
	reverse	TCACTGTCCCAGCATCTTGT
IL6	forward	ACCACGGCCTTCCCTACTTC
	reverse	CATTTCCACGATTTCCCAGA
IL1β	forward	TTCAGGCAGGCAGTATCACTC
	reverse	GAAGGTCCACGGGAAAGACAC
CCL2	forward	TAAAAACCTGGATCGGAACCAAA
	reverse	GCATTAGCTTCAGATTTACGGGT
CCR2	forward	CCTCAGTTCATCCACGGCAT
	reverse	AGGGAGTAGAGTGGAGGCAG
OPN	forward	CCGAGGTGATAGCTTGGCTTAT
	reverse	ATGGCTGCCCTTTCCGTTGTTG
AT1R	forward	GTAATGCCCTGACAGAAACCA
	reverse	AAACCCACAAATCCATCCAG
PPARγ	forward	GGAGCCTAAGTTTGAGTTTGC
	reverse	GACGATCTGCCTGAGGTCTG
PPARα	forward	GCTGCTATAATTTGCTGTGGA
	reverse	CTTTGGGAAGAGGAAGGTGT
EMMPRIN	forward	CAGTGGTGGTTTGAAGGGAATGC
	reverse	TGGGTGGCCGAGTAAGGTGGTT
MMP2	forward	GACACCTGGTTTCACCCTTTC
	reverse	TCAGACAACCCGAGTCCTTT
MMP9	forward	TGGTCTTCCCCAAAGACCTG
	reverse	CACAGCGTGGTGTTCGAATG
MMP3	forward	TGCATGACAGTGCAAGGGAT
	reverse	GGGAAGGTACTGAAGCCACC
MMP12	forward	GGCTGCTCCCATGAATGACA
	reverse	GTACATCGGGCACTCCACAT
MMP13	forward	TACCATCCTGCGACTCTTGC
	reverse	TTCACCCACATCAGGCACTC
TIMP1	forward	CCCCAGTCATGGAAAGCC
	reverse	GCCAGGGAACCAAGAAGC
CTSS	forward	ACCTGGTGGACTGCTCAAAT
	reverse	GGAAGCGTCTGCCTCTATGC
CTSL	forward	AGGAATTCAGGCAGGTGGTG
	reverse	CGCTAAACGCCCAACAAGAC
CTSK	forward	GACACCCAGTGGGAGCTATG
	reverse	AGTGGTTCATGGCCAGTTCA
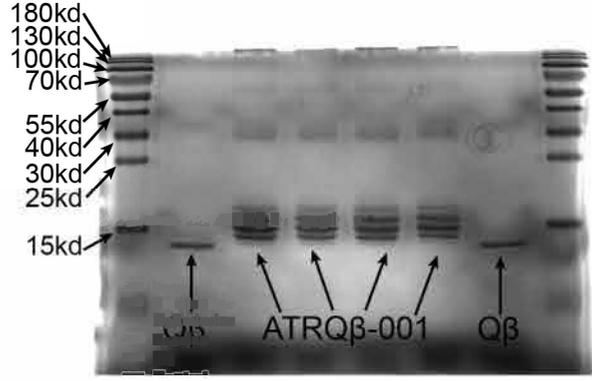
Figure S1

The vaccine was analyzed on an SDS-PAGE gel. The figure showed the ATRQβ-001 peptides conjugated to the Qβ VLP
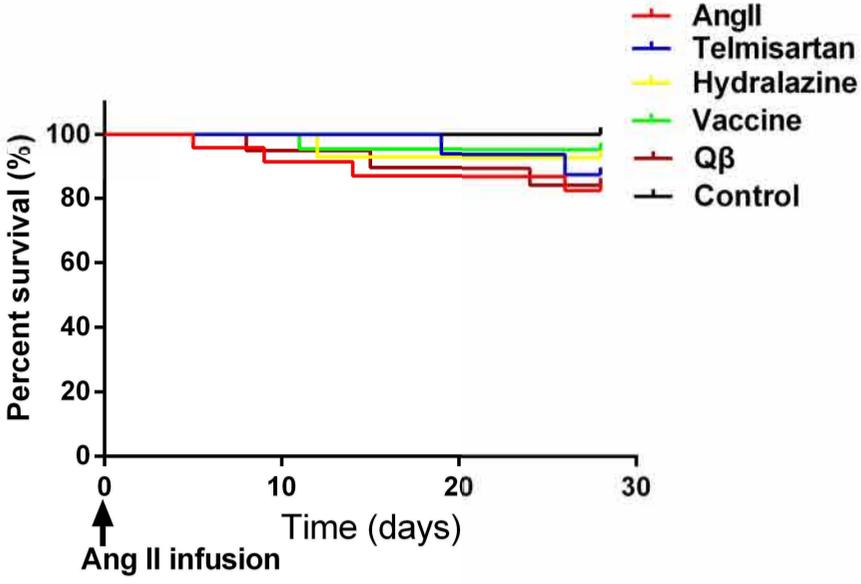
Figure S2

Kaplan-Meier survival curve shows survival rates at 28 days were 82.6% for the Ang II group, 87.5% for the Telmisartan group, and 92.86% for the Hydralazine group, 95.23% for the Vaccine group, 85% for the Qβ group, 100% for the Control group. Number of mice: Ang II n=23, Telmisartan n=16, Hydralazine n14, Vaccine n=21, Qβ n=20, Control n=8.
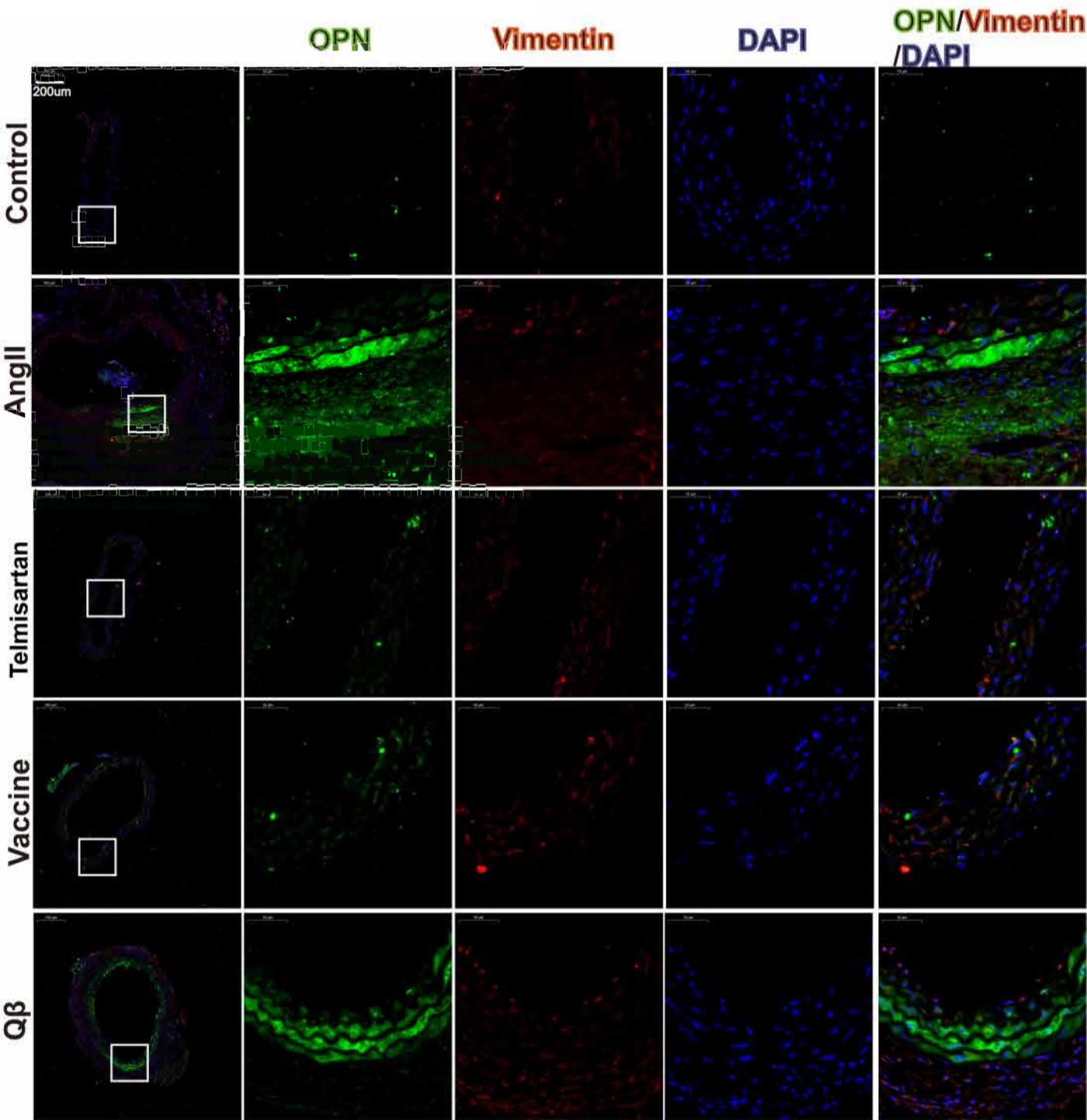
Figure S3

Expression of sections of OPN (green) and vimentin (red) on abdominal aorta sections on 7 days post Ang II infusion were detected by immunofluorescence, Scale bar represents 200μm. OPN, osteopontin
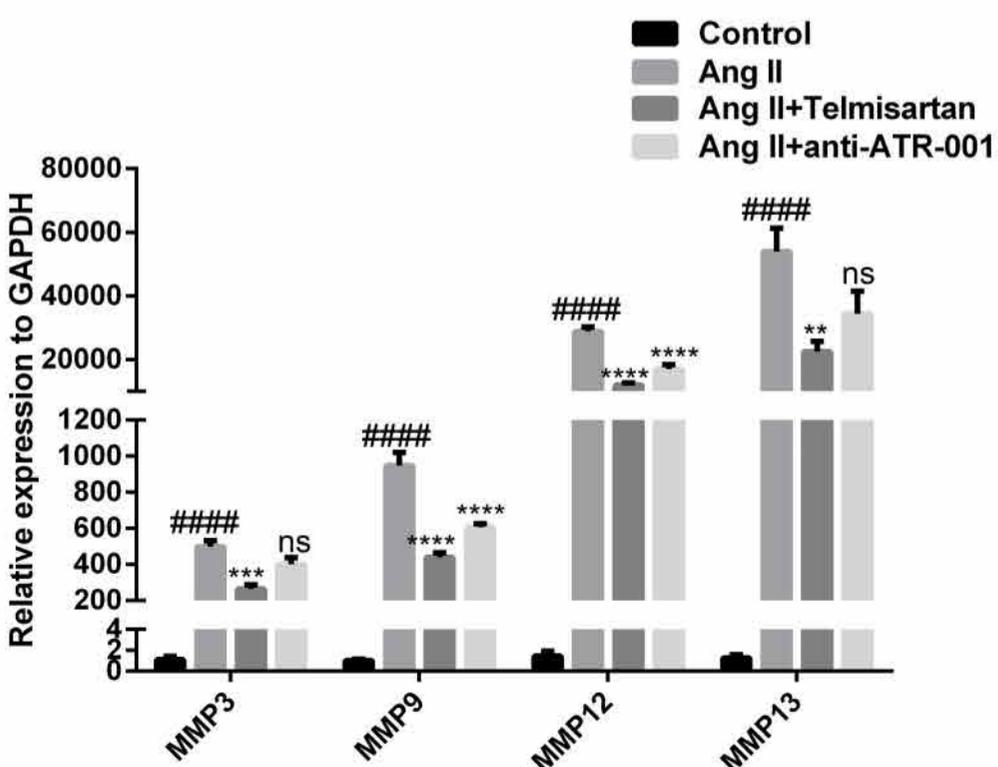
Figure S4

The anti-ATR-001 antibody inhibited LPS-induced MMPs transcription in macrophage. RAW264.7 cells were pretreated with the anti-ATR-001 antibody (10μg/ml), telmisartan (1*10^−6mol/l), or the NATR for 2 h respectively, and then incubated with LPS (0.5μg/ml) for 24 h. The relative mRNA expression of MMPs detected by quantitative real-time PCR.

Data are expressed as means ± SEM. **P<0.01, ***P<0.001, ****P<0.0001 vs. the LPS group; ####P<0.0001 vs. the Control group.